

A numerical damped oscillator approach to constrained Schrödinger equations

M. Ögren*

*School of Science and Technology, Örebro University, 701 82 Örebro, Sweden, and
Hellenic Mediterranean University, P.O. Box 1939, GR-71004, Heraklion, Greece.*

M. Gulliksson†

*School of Science and Technology, Örebro University, 701 82 Örebro, Sweden, and
Institutt for data og realfag, Høgskulen på Vestlandet, 5020 Bergen, Norway.*

(Dated: June 29, 2022)

Abstract

This article explains and illustrates the use of a set of coupled dynamical equations, second order in a fictitious time, which converges to solutions of stationary Schrödinger equations with additional constraints. We include three qualitative different numerical examples: the radial Schrödinger equation for the hydrogen atom; the two-dimensional harmonic oscillator with degenerate excited states; and finally a non-linear Schrödinger equation for rotating states. The presented method is intuitive, with analogies in classical mechanics for damped oscillators, and easy to implement, either in own coding, or with software for dynamical systems. Hence, we find it suitable to introduce it in a continuation course in quantum mechanics or generally in applied mathematics courses which contain computational parts.

I. INTRODUCTION

In this article we describe the idea of solving stationary Schrödinger equations (SE) as energy minimization problems with constraints, by using a second order damped dynamical system. We discuss how to numerically solve the problems in a stable and efficient way.

For the formulas of this article to be easily recognised and directly applicable for the students of different courses, we write out most formulas explicitly in an infinite-dimensional representation. For example, we use integrals instead of scalar products (or Dirac notation). However, if you write your own code¹ instead of using high-level solvers for the differential equations, you need to formulate integrals as finite sums and derivatives, e.g., as finite differences, i.e., the linear Schrödinger equation can be formulated as a linear matrix equation $Hu = Eu$, with H a matrix, u a (column) eigen-vector, and E an eigenvalue of H . We provide enough details, including the references, for all the numerical results presented here to be reproducible. From a pedagogical point of view, the method has the advantage of being able to solve a large set of problems with the same main idea and high-level software as well as incorporating several important concepts from classical mechanics. We hope the readers will expand the theory and applications in different directions from the examples presented here.

II. THE METHOD

In order to introduce the idea of the method let us first consider a basic example in classical mechanics. The harmonic oscillator is according to Newton's second law described by

$$M\ddot{u} + ku = 0, \quad k > 0. \quad (1)$$

Here $u = u(t)$ is the distance from the equilibrium for a mass M on which a force $-ku$ is acting. The dot denotes the time derivative. For example the mass could be attached to a spring, with k being the spring constant, see Fig. 1. If we in addition assume that there is some friction force proportional to the velocity \dot{u} , e.g., between the mass and the surface on which it is sliding, we get a damped second order system

$$M\ddot{u} + \eta\dot{u} + ku = 0, \quad (2)$$

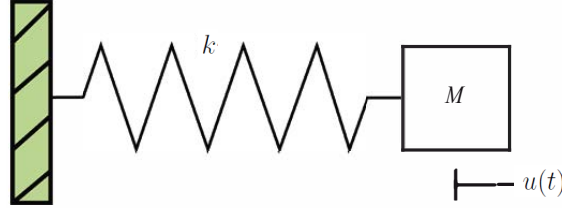


FIG. 1. A simple oscillating spring-mass system.

where $\eta > 0$ is a damping parameter due to the friction. It is clear from this example that one of the parameters M , η , k can be scaled out, so we usually set $M = 1$ in the following. The solutions of Eq. (2) in the non-critical case ($\eta \neq 2\sqrt{k}$) are given by

$$u(t) = C_1 \exp(\xi_1 t) + C_2 \exp(\xi_2 t), \quad (3)$$

where C_i are determined by the initial conditions $u(0)$ and $\dot{u}(0)$, and $\xi_j = -\eta/2 \pm \sqrt{(\eta/2)^2 - k}$. It is easy to see from Eq. (3) that u tends to zero for large times, which is the equilibrium position of the mass and hence the stationary solution to Eq. (2). The value $\eta = 2\sqrt{k}$ for the damping parameter ensures the ξ_j to be real and is referred to as critical damping for Eq. (2), for which $u(t) = (C_1 + C_2 t) \exp(-\sqrt{k}t)$. For smaller or larger values of η , the oscillations are referred to as under- or over-damped respectively. The critically damped system is known to be the fastest way for the system to return to its equilibrium, i.e., to reach the stationary solution. In multimode discretized systems the above argument can be generalized in order to obtain an optimal value for the damping parameter to be used in a numerical calculation².

Now we note that $u = 0$ is also the solution of the (trivial) minimization problem $\min(ku^2/2)$. In fact, the convex functional $V(u) = ku^2/2$ is the mechanical potential corresponding to the force $F = -ku$ which is conservative since $F = -dV/du$. Of course, in this case it is easier to directly solve $ku = 0$ or $\min ku^2/2$ for u , than to integrate the differential equation (2). However, this simple idea can be extended to solve more challenging problems, where η takes the role of a parameter that can be tuned for optimal numerical properties, as we explain in this article.

A. Damped oscillator approach to the groundstate of the Schrödinger equation

We here briefly repeat that the stationary (i.e., time-independent) SE for a particle with mass M and a spatially-dependent potential $V(\mathbf{r}, t) = V(\mathbf{r})$ follows from the time-dependent SE

$$i\hbar \frac{\partial \Psi}{\partial t} = -\frac{\hbar^2}{2M} \nabla^2 \Psi + V\Psi \equiv \hat{H}\Psi. \quad (4)$$

Given a time and space separating ansatz of the wavefunction $\Psi(\mathbf{r}, t) = \varphi(\mathbf{r}) \exp(-iEt/\hbar)$, we then have from Eq. (4)

$$\hat{H}u = Eu. \quad (5)$$

Alternatively, the SE can be viewed as the Euler-Lagrange equation³ corresponding to the minimization of the energy, which if we start from Eq. (5) is the following functional of u

$$E(u) = \frac{\int \bar{u} \hat{H} u d\mathbf{r}}{\int |u|^2 d\mathbf{r}}, \quad (6)$$

where the bar from now on denotes complex conjugation.

If the normalization of the wave function is considered as a constraint, then the denominator of Eq. (6) is unity and we can write for the groundstate of Eq. (5)

$$E = \min_u \int \bar{u} \hat{H} u d\mathbf{r}, \text{ s.t. } \int |u|^2 d\mathbf{r} = 1, \quad (7)$$

where *s.t.* is an abbreviation for *subject to*. We later also give examples with more complicated constraints.

The main idea now for solving Eq. (7), already introduced above, is to utilize the fact that the solution to Eq. (7) is also a stationary solution, say $u^*(\mathbf{r})$, to the second order damped dynamical system

$$\ddot{u} + \eta \dot{u} + \frac{\delta E}{\delta \bar{u}} = 0, \eta > 0, \int |u|^2 d\mathbf{r} = 1, \quad (8)$$

where we in the following reserve the dot notation for the derivatives with respect to a fictitious time τ . The term $\delta E / \delta \bar{u}$ above is a functional derivative of the energy, such that $u(\tau) \rightarrow u^*$ will satisfy the Euler-Lagrange equation $\delta E / \delta \bar{u} = 0$ when $\tau \rightarrow \infty$. The corresponding energy is $E(u^*) = \min_u \left(\int \bar{u} \hat{H} u d\mathbf{r} \right)$ where \hat{H} is the Hamiltonian operator from the SE (4). The solution of Eq. (8) is unique and globally stable, see e.g. references in⁴.

After the problem has been formulated as in Eq. (8), an important question is the following: How does one choose a stable and efficient numerical method⁵ for obtaining the stationary solution to Eq. (8)? Symplectic integration methods are tailor-made for Hamiltonian systems. This serves as the motivation for our choice of numerical method. Let us rewrite Eq. (8) as the first order system

$$\begin{aligned}\dot{u} &= v \\ \dot{v} &= -\eta v - \frac{\delta E}{\delta \bar{u}}.\end{aligned}\tag{9}$$

Then, we can apply a symplectic explicit method, such as symplectic Euler or Störmer-Verlet⁵, which give us an iterative map in the numerical approximations (u_ν, v_ν) , $\nu = 1, 2, 3, \dots$ with a step in fictitious time $\Delta\tau_\nu$ and a damping η_ν . The choice of parameters $\Delta\tau_\nu$ and η_ν can be aimed to optimize the performance of the numerical method, which generally is a non-trivial task. But for linear differential equations, such as the Schrödinger equation, analytic results exist^{2,6}. For simplicity we here keep all parameters constant through the iterations, i.e., independent of the step ν .

The approach of finding the solution to Eq. (7) by solving Eq. (8) with a symplectic method has been named the *dynamical functional particle method* (DFPM)⁷. We would like to emphasize that it is the combination of the second order damped dynamical system together with an efficient (fast, stable, accurate) symplectic solver that makes DFPM a very powerful method. Even if the idea of solving minimization problems using dynamical systems with different damping strategies goes far back, see Refs.^{8,9}, it has not been presented for the Schrödinger equation with constraints with symplectic solvers for second order systems. According to our practical experience many common (non-symplectic) integration methods with optimal or non-optimal damping parameters give a reasonably fast convergence of Eq. (8) to the stationary solutions. So unless the numerical performance is important, a variety of softwares¹ for dynamical systems can be used in practical implementations.

Let us finally comment on one specific closely related approach for solving Eq. (7) that has been studied extensively^{10,11}. The steepest descent method

$$\dot{u}(t) + \alpha \frac{\delta E}{\delta \bar{u}} = 0, \alpha > 0, \int |u|^2 d\mathbf{r} = 1,\tag{10}$$

often called *the imaginary time method* when applied for the SE with $\alpha = 1$ (i.e., change $t \rightarrow -i\tau$ in Eq. (4)). It might seem that Eq. (10) should serve better than Eq. (8) since

the exponential decrease towards the stationary solution in Eq. (10) can be made arbitrary large by choosing α large enough.

However, as proved strictly for linear problems², and by numerical evidence for some non-linear examples¹², going to a second order differential equation in a fictitious time is superior if one takes into account the stability and accuracy of the numerical solver. DFPM has been shown to have a remarkably faster convergence to the stationary solution than any numerical method applied to Eq. (10), see².

It is the purpose of this article to explain this new method through a few qualitatively different examples for the stationary SE. In addition it will be extended to a corresponding method to treat constraints.

B. Damped oscillator approach for global constraints

Common methods for calculating excited states are so called shooting methods¹³, although restricted to systems in one spatial dimension or with potentials obeying separation of variables and methods based on diagonalization¹⁴.

DFPM is readily extended to more general constrained problems, e.g., needed for finding normalized- and excited states of the SE in general settings. Consider a convex minimization problem for $E(u)$ with smooth global constraint functionals $G_j(u) = 0$, i.e.,

$$\min_u E(u), \text{ s.t. } G_j(u) = 0, \quad j = 1, 2, 3, \dots . \quad (11)$$

The problem in Eq. (11) has a unique solution u^* if $\delta G_j / \delta \bar{u}$ is surjective at u^* , and thus it fulfills a so-called Karush-Kuhn-Tucker condition. The corresponding dynamical system for constraints can be formulated using an extended constrained energy functional (often called Lagrange function in mathematical literature) $I(u, \mu_1, \mu_2, \dots) = E(u) + \sum_j \mu_j G_j(u)$, where μ_j are Lagrange multipliers. The dynamical system for solving Eq. (11) is then given by

$$\ddot{u} + \eta \dot{u} + \frac{\delta E}{\delta \bar{u}} + \sum_j \mu_j \frac{\delta G_j}{\delta \bar{u}} = 0, \quad (12)$$

with $\mu_j(\tau)$ chosen such that $u(\tau)$ tends to u^* during the evolution, see examples in the next section. For more details on existence and uniqueness of solutions to constrained problems see¹⁵ and references therein.

In order to solve Eq. (11) one can choose the $\mu_j(\tau)$ such that $u(\tau)$ always remains on the constraints set, e.g., by projection methods, or as we will do here to approach it (oscillatorily) as τ grows. Projection is generally costly but there are important exceptions such as, e.g., eigenvalue problems with only normalization constraints.

For our damped approach, we introduce an additional dynamical system, analogous to Eqs. (2) and (8), for a constraint G_j as in Eq. (11) according to

$$\ddot{G}_j + \eta \dot{G}_j + k_j G_j = 0, \quad \eta > 0, \quad k_j > 0, \quad j = 1, 2, 3, \dots . \quad (13)$$

Then $G_j(u(\tau))$ tends to zero exponentially fast and the equations (13) can be used to derive expressions of the Lagrange multipliers $\mu_j(\tau)$ for Eq. (12), which for some problems are explicit.

This method was introduced in⁶ for solving matrix eigenvalue problems, where it was shown that $u(\tau)$ converges asymptotically to the eigenvectors. It was also shown that the choice of k_j in Eq. (13) does not change the local convergence rate if k_j lie within a rather large range which is determined by the eigenvalues to the operator $\delta E / \delta \bar{u}$, see⁶ for details. In this article we always keep $k_j = k$ for all j for simplicity, while using the freedom in different k_j can further improve the numerical performance of the method. Under these assumptions, the local convergence rate of the corresponding symplectic Euler with the optimal parameters² will be the same as for the projection approach. However, while the two approaches have the same local behaviour it is not generally a priori known which of these two methods is faster for a specific problem. A general known disadvantage with projection is that large changes in the Lagrange multipliers require small timesteps.

III. CONSTRAINTS FOR THE EXCITED STATES OF THE SCHRÖDINGER EQUATION

In the numerical examples to be presented in Sections IV A and IV B, both a normalization constraint and several orthogonalization constraints are treated simultaneously. We start to derive the Lagrange multiplier for only a normalization constraint in detail, then we add only one orthogonalization constraint, i.e., what is needed to calculate the first excited state of the SE. In Appendix A, we show how an arbitrary number of orthogonalization constraints are treated.

A. Normalization constraint

Taking the first and second order derivatives of the normalization constraint

$$G_1 = 1 - \int |u|^2 d\mathbf{x} \equiv 1 - N(\tau) = 0, \quad (14)$$

with respect to τ gives

$$\dot{G}_1 = - \int (\dot{u}u + \bar{u}\dot{u}) d\mathbf{x}, \quad \ddot{G}_1 = - \int (\ddot{u}u + 2\dot{u}\dot{u} + \bar{u}\ddot{u}) d\mathbf{x}. \quad (15)$$

Inserting the expressions from Eq. (15) into the left hand side of the general differential equation for constraints (13), then gives after simplifications

$$\ddot{G}_1 + \eta \dot{G}_1 = - \int (\{\ddot{u} + \eta \dot{u}\} u + \bar{u} \{\ddot{u} + \eta \dot{u}\} + 2|\dot{u}|^2) d\mathbf{x}. \quad (16)$$

If we now use the DFPM equation (12) with $\delta E/\delta \bar{u} + \mu_1 \delta G_1/\delta \bar{u} = \hat{H}u - \mu_1 u$ for the stationary SE, we can identify the limit of the Lagrange multiplier being equal to the energy $\lim_{\tau \rightarrow \infty} \mu_1(\tau) = E$ in this case, compare with Eq. (5). Inserting $-\hat{H}u + \mu_1 u$ into the curly brackets of Eq. (16) gives after simplifications

$$\ddot{G}_1 + \eta \dot{G}_1 = 2E - 2\mu_1 N - 2 \int |\dot{u}|^2 d\mathbf{x} = -k_1 (1 - N), \quad (17)$$

with $E(\tau) \equiv \int \bar{u} \hat{H} u d\mathbf{x}$. Finally we can solve for the Lagrange multiplier $\mu_1(\tau)$

$$\mu_1 = \frac{E + k_1 (1 - N) / 2 - \int |\dot{u}|^2 d\mathbf{x}}{N}. \quad (18)$$

We see in Eq. (18) that $\mu_1 \rightarrow E$, since $|\dot{u}| \rightarrow 0$, $N \rightarrow 1$ as $\tau \rightarrow \infty$.

B. Normalization constraint and one orthogonalization constraint

Introducing, in addition to G_1 above, the following orthogonalization constraint

$$G_0 = \int \bar{u} u_0 d\mathbf{x} = 0, \quad (19)$$

means that the solution u , should be orthogonal to a known normalized function u_0 . This u_0 can be defined analytically, which can be helpful while testing software¹, but more often u_0 is a numerically obtained solution. For example in the case of a convex 1D problem, u_0 is the solution with the lowest eigenvalue E (groundstate), and u is the solution with the

second lowest eigenvalue E (first excited state). As seen in the 2D example of Sec. IV B, this situation can be more complicated in higher dimensions where eigenvalues can be degenerate, meaning that several different solutions can have the same eigenvalue.

Taking the first and second order derivatives with respect to τ of the orthogonalization constraint in Eq. (19) gives

$$\dot{G}_0 = \int \dot{u} u_0 d\mathbf{x}, \quad \ddot{G}_0 = \int \ddot{u} u_0 d\mathbf{x}. \quad (20)$$

Inserting the expressions from Eqs. (19) and (20) into the general differential equation for constraints (13), then gives with simplifications

$$\ddot{G}_0 + \eta \dot{G}_0 = \int \{\ddot{u} + \eta \dot{u}\} u_0 d\mathbf{x} = \int \{-\hat{H} \bar{u} + \mu_1 \bar{u}\} u_0 d\mathbf{x} - \mu_0 = -k_0 G_0. \quad (21)$$

In comparison to Eq. (17) there is now an additional term ($j = 0$) in Eq. (12). The corresponding coupled equation for G_1 is now

$$\ddot{G}_1 + \eta \dot{G}_1 = 2E - 2\mu_1 N + \int (\mu_0 \bar{u}_0 u + \mu_0 \bar{u} u_0 - 2|\dot{u}|^2) d\mathbf{x} = -k_1 G_1. \quad (22)$$

Finally we write Eqs. (21) and (22) for the two coupled Lagrange multipliers $\mu_0(\tau)$ and $\mu_1(\tau)$ as a linear system

$$\begin{bmatrix} 1 & -G_0 \\ -\text{Re}(G_0) & 1 - G_1 \end{bmatrix} \begin{bmatrix} \mu_0 \\ \mu_1 \end{bmatrix} = \begin{bmatrix} k_0 G_0 - \int u_0 \hat{H} \bar{u} d\mathbf{x} \\ E - \int |\dot{u}|^2 d\mathbf{x} + k_1 G_1 / 2 \end{bmatrix} \equiv \begin{bmatrix} y_1 \\ y_2 \end{bmatrix}, \quad (23)$$

where $\text{Re}(G_0) = \int (\bar{u}_0 u + \bar{u} u_0) d\mathbf{x} / 2$. Again, we can check the limits for the Lagrange multipliers from Eq. (23), i.e., $\mu_0 \rightarrow 0$ and $\mu_1 \rightarrow E$, since $\dot{u} \rightarrow 0$, $G_0 \rightarrow 0$, $G_1 \rightarrow 0$ as $\tau \rightarrow \infty$.

Using Cramer's rule on the linear system of Eq. (23) give the explicit expressions

$$\mu_0 = \frac{(1 - G_1)y_1 + G_0 y_2}{(1 - G_1) - G_0 \text{Re}(G_0)}, \quad \mu_1 = \frac{y_2 + \text{Re}(G_0) y_1}{(1 - G_1) - G_0 \text{Re}(G_0)}, \quad (24)$$

that can be used to calculate the first excited state in various problems. We give two such specific examples in the next section.

IV. NUMERICAL EXAMPLES

In this section we show numerical results using the symplectic Euler method⁵ for three examples and compare the presented DFPM method against analytic formulas. The first

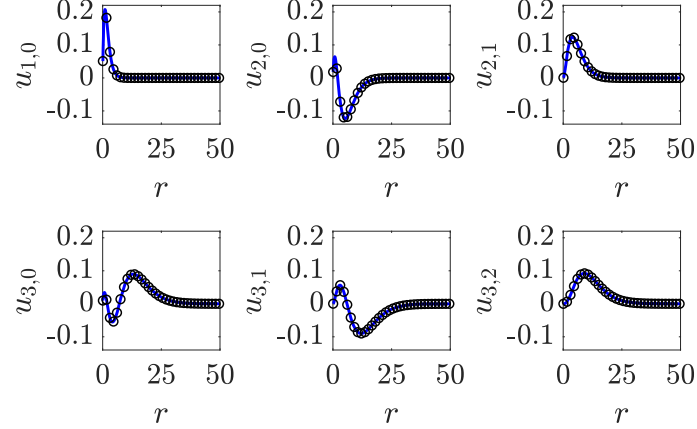


FIG. 2. The six numerical solutions of Eq. (28) with the lowest energies E . Solid (blue) curves are numerical results, while (black) circles show the result of Eq. (27). We used an equidistant grid $10^{-6} < r_j < 10^2$, $j = 1, \dots, 10^3$, and τ_{\max} large enough such that $|\ddot{u} + \eta \dot{u}| < 10^{-6}$ in Eq. (12). DFPM parameters used were $\eta = 0.5$, $k = 4$, and $\Delta\tau = 0.1$, which are of the same order of magnitude as the optimal predicted values for linear systems². The (real) initial condition $u(0)$ was in this example chosen randomly. We note that the sign of the final wavefunction depends on the initial condition used.

example is a linear equation in one radial variable for the hydrogen atom. The second is a harmonic oscillator in two variables (2D), which gives degenerated energies. Finally, an example of a non-linear Schrödinger equation is given.

A. The radial equation for the hydrogen atom

The function u , is in this example the radial part of the three-dimensional spatial wavefunction from Eq. (4) multiplied with the radius $r = |\mathbf{r}|$, i.e., $\varphi(\mathbf{r}) = \varphi(r, \theta, \phi) = u(r)/r Y_l^m(\theta, \phi)$. We write the dimensionless (i.e., with $\hbar = M_e = a_0 = 1$) radial SE of the hydrogen atom as

$$\hat{H}_{(r)} u(r) \equiv -\frac{1}{2} \frac{\partial^2 u}{\partial r^2} + \left(\frac{l(l+1)}{2r^2} - \frac{1}{r} \right) u = Eu, \quad 4\pi \int_0^\infty |u|^2 dr = 1, \quad (25)$$

where the expression within the large parenthesis above is referred to as the effective radial potential. For comparison, the energies only depend on a single quantum number $n =$

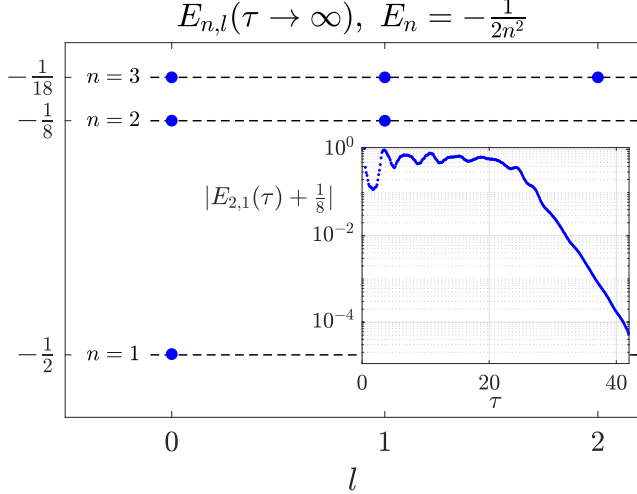


FIG. 3. The six lowest energies E for the hydrogen atom. Dots (blue) are the numerically calculated energies from Eq. (28). The dashed horizontal (black) lines correspond to the values from Eq. (26). The inset figure shows the convergence dynamics of the energy $E_{2,1}$ as function of the fictitious time. The parameters used are reported in Fig. 2.

1, 2, 3, ... and are given by¹⁶

$$E_n = -\frac{M_e e^4}{2(4\pi\epsilon_0)^2 \hbar^2} \frac{1}{n^2} = -\frac{\hbar^2}{2M_e a_0^2} \frac{1}{n^2} = -\frac{1}{2} \frac{1}{n^2}, \quad (26)$$

where $a_0 = 4\pi\epsilon_0\hbar^2/(M_e e^2)$ is a length scale called the Bohr radius. The corresponding radial wavefunctions depend on the two quantum numbers $n = 1, 2, 3, \dots$ and $l = 0, 1, 2, \dots, n-1$ and are given by¹⁶

$$u_{n,l}(r)/r = \sqrt{\frac{1}{\pi a_0^3 n^4} \frac{(n-l-1)!}{(n+l)!}} \left(\frac{2r}{na_0}\right)^l L_{n-l-1}^{2l+1} \left(\frac{2r}{na_0}\right) \exp\left(-\frac{r}{na_0}\right), \quad (27)$$

where L denotes the generalized Laguerre polynomials¹⁷.

The effective potential in Eq. (25) depends on the quantum number l , as do the solutions in Eq. (27), so there is not any degeneracy when solving Eq. (25) numerically. In other words, the solution u is unique for this radial SE. However, all states with the same quantum number n have the same energy E , as is clear from Eq. (26), and together with the degeneracy $(2m+1)$ for the so called spherical harmonics Y_l^m , the three-dimensional wavefunction for Hydrogen have a n^2 degeneracy.

For the numerical approach, the solutions $u_{n,l*}$ with $n = 1, 2, \dots, n^* - 1$ should be orthogonal to the unknown $u_{n^*,l*}$. Since one needs access to $u_{n,l*}$, $n = 1, 2, \dots, n^* - 1$ to obtain $u_{n^*,l*}$,

we solve Eq. (12) in consecutive order. This means first only with a normalization constraint, see Sec. III A, to obtain u_{1,l^*} , then with one additional orthogonality constraint, see Sec. III B, to obtain u_{2,l^*} , and then with several orthogonality constraints, see Appendix A, to obtain the solutions u_{n^*,l^*} with $n^* > 2$.

We can write the n^* different constraints compactly using the Kronecker delta according to $G_n = 4\pi \int_0^\infty \bar{u}_{n^*,l^*} u_{n,l^*} dr - \delta_{n^*,n} = 0$, $n = 1, 2, \dots, n^*$. Using Eq. (25) we formulate the dynamical system, different for each value of l^* , that is Eq. (12) applied to this radial SE is

$$\ddot{u}_{n^*,l^*} + \eta \dot{u}_{n^*,l^*} + \hat{H}_{(r)}(l^*) u_{n^*,l^*} + \sum_{n=1}^{n^*} \mu_n \frac{\delta G_n}{\delta \bar{u}} = 0. \quad (28)$$

The two Lagrange multipliers needed in the sum above to calculate the first excited state, i.e. for $n^* = 2$, can be obtained from Eq. (24). For the case with several multipliers ($n^* > 2$) in Eq. (28), they can conveniently be obtained from e.g. numerical solutions of Eq. (A6).

The six stationary numerical solutions to Eq. (28) with lowest energies are plotted in Fig. 2, while the corresponding energies are illustrated in Fig. 3.

B. Two-dimensional harmonic oscillator

In this example we calculate the well known wave functions $u(x, y)$ and energies E to the dimensionless (i.e., with $\hbar = M = \omega = 1$) Schrödinger equation with an isotropic two-dimensional harmonic potential on a 2D Cartesian grid

$$\hat{H}u \equiv -\frac{1}{2} \left(\frac{\partial^2}{\partial x^2} + \frac{\partial^2}{\partial y^2} \right) u + \frac{1}{2} (x^2 + y^2) u = Eu, \quad \int_{\mathbb{R}^2} |u|^2 d\mathbf{r} = 1. \quad (29)$$

That is, for the groundstate we solve the following optimization problem

$$\min_u \int_{\mathbb{R}^2} \bar{u} \hat{H} u d\mathbf{r}, \text{ s.t. } \int_{\mathbb{R}^2} |u|^2 d\mathbf{r} = 1.$$

Let u_s denote the s 'th eigenstate and $E_s = \int_{\mathbb{R}^2} \bar{u}_s \hat{H} u_s d\mathbf{r}$ the corresponding eigenvalue. To obtain u_{s^*} for $s^* > 1$ we use, in addition to Eq. (29), the $s^* - 1$ orthogonality constraints

$$\int_{\mathbb{R}^2} \bar{u}_{s^*} u_1 d\mathbf{r} = 0, \int_{\mathbb{R}^2} \bar{u}_{s^*} u_2 d\mathbf{r} = 0, \dots, \int_{\mathbb{R}^2} \bar{u}_{s^*} u_{s^*-1} d\mathbf{r} = 0. \quad (30)$$

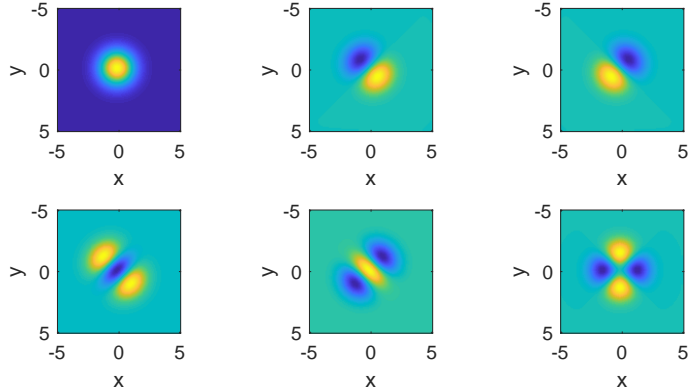


FIG. 4. The six numerical wavefunctions of Eq. (31), with the lowest energies E . The color coding is bright (yellow) for the largest positive values in each subfigure, and dark (blue) for the lowest values. We used $-5 \leq x, y \leq 5$ and $\Delta x = \Delta y = 1/12$ for the discretization, which is enough to obtain all six solutions with correct energies within 3 significant digits, see Eq. (32). The parameters were $\eta = 1.5$, $k = 0.5$ and $\Delta\tau = 0.05$, which is in the same order of magnitude as predicted to be optimal². The initial wavefunction (for all six subfigures here) was a translated and scaled (unnormalized) Gaussian $u(\tau = 0) = 1.2/\sqrt{\pi} \exp(-((x - 1.2)^2 + (y - 1.2)^2)/2)$ with $E(\tau = 0) \simeq 2.5$ (see the left ring in Fig. 5). The six numerical wavefunctions, from the upper left subfigure to the bottom right subfigure, corresponds to $u_{(n_x, n_y)}$ from Eq. (32) in the order $(n_x, n_y) = (0, 0), (1, 0), (0, 1); (2, 0), (0, 2), (1, 1)$. However, we note that the orientation and phase (sign) of the final wavefunction depends on the initial condition used.

Using Eqs. (29) and (30) we can from Eq. (12) formulate the corresponding dynamical system with the s^* constraints $G_s = \int_{\mathbb{R}^2} \bar{u}_{s^*} u_s d\mathbf{r} - \delta_{s^*, s} = 0$, $s = 1, 2, \dots, s^*$, as

$$\ddot{u}_{s^*} + \eta \dot{u}_{s^*} + \hat{H} u_{s^*} + \sum_{s=1}^{s^*} \mu_s \frac{\delta G_s}{\delta \bar{u}} = 0. \quad (31)$$

Since one needs access to u_s , $s = 1, 2, \dots, s^* - 1$, we solve Eq. (31) in consecutive order. The two Lagrange multipliers needed in the sum above to calculate the first excited state, i.e. for $s^* = 2$, are given by Eq. (24). For the case with several multipliers ($s^* > 2$) in Eq. (31), see Appendix A, they can conveniently be obtained from e.g. numerical solutions of Eq. (A6). We show the six first numerical solutions to Eq. (31) in Fig. 4.

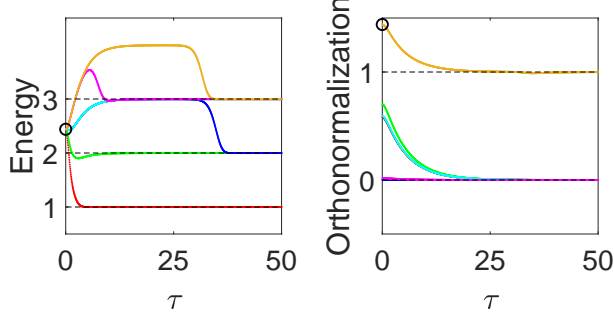


FIG. 5. Left figure: Convergence of the energies for the six solutions seen in Fig. 4. Dashed horizontal lines correspond to the exact energies of Eq. (32). Right figure: Illustration of the convergence of the calculation for solution number six (i.e. $s^* = 5$ corresponding to $n_x = n_y = 1$). The most upper curve show the normalization $\int |u|^2 d\mathbf{r}$ (the ring shows the value $1.2^2 = 1.44$, see the initial condition in the caption of Fig. 4), and the lower curves shows the five orthogonality constraints $\int \bar{u} u_s d\mathbf{r}$, $s = 0, 1, 2, 3, 4$.

For comparisons we note that the equation (29) possesses the explicit solutions¹⁶

$$E_{(n_x, n_y)} = n_x + n_y + 1, \quad u_{(n_x, n_y)}(x, y) = \frac{1}{\sqrt{2^{(n_x+n_y)} n_x! n_y! \pi}} \mathcal{H}_{n_x}(x) \mathcal{H}_{n_y}(y) \exp\left(-\frac{x^2 + y^2}{2}\right), \quad (32)$$

where \mathcal{H} denote the Hermite polynomials¹⁷, and the two quantum numbers can take the values $n_x, n_y = 0, 1, 2, 3, \dots$.

In contrast to the radial SE for the hydrogen atom, there is no dependence on any of the quantum numbers n_x, n_y in the SE (29), and different solutions $u_{(n_x, n_y)}$ give degenerate energies $E_{(n_x, n_y)}$ as long as $n_x + n_y = \text{constant}$, see Eq. (32).

In the left plot of Fig. 5 we show the numerical convergence for the energies. In the right plot of Fig. 5 we show the numerical convergence for the constraints.

C. The non-linear Schrödinger equation under rotation

The non-linear Schrödinger equation (NLSE) is commonly used to model, many interacting bosonic particles via a mean-field approximation¹⁸. We have developed a DFPM formulation with damped constraints for a dimensionless non-linear Schrödinger equation in $u = u(x)$ on a ring geometry $-\pi \leq x \leq \pi$ (with radius $R = \hbar = 2M = 1$) using periodic boundary conditions $u(-\pi) = u(\pi)$.

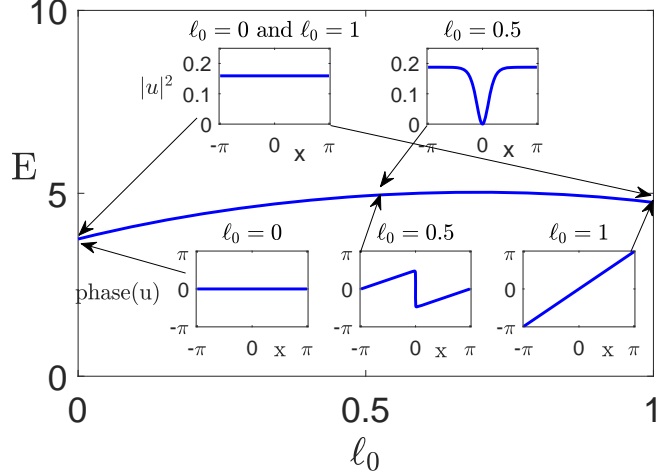


FIG. 6. Yrast curve¹², i.e. energy vs momentum, with some examples of the density and the phase for the wavefunction u for the constant of non-linearity being $\gamma = 7.5$. Optimal numerical parameters in Eq. (35) are not trivially given in the non-linear case, and we used $\eta = k/2 = 1$ and $\Delta\tau = 0.015$. The spatial equidistant discretization used 400 points

The aim is to minimize the total energy

$$E(u) = \int_{-\pi}^{\pi} \left| \frac{\partial u}{\partial x} \right|^2 + \pi\gamma |u|^4 dx, \quad (33)$$

subject to one constraint for normalization, and one constraint for the angular momentum being ℓ_0

$$G_1 = 1 - \int_{-\pi}^{\pi} |u|^2 dx = 0, \quad G_2 = \ell_0 + i \int_{-\pi}^{\pi} \bar{u} \frac{\partial u}{\partial x} dx = 0. \quad (34)$$

We note that this problem can be solved analytically and refer to Appendix B of Ref.¹² for the details of the solutions. In earlier work we implemented DFPM numerically for this problem with a modified RATTLE method¹², in which we solved for the two Lagrange multipliers corresponding to Eq. (34) numerically in each timestep. There it was demonstrated that DFPM outperformed another commonly used method that is first order in time¹². In this article we instead couple the minimization of Eq. (33) to Eq. (34), via the dynamical equations for the constraints and get the following realization of Eq. (12)

$$\ddot{u} + \eta \dot{u} + \frac{\delta E}{\delta \bar{u}} + \mu \frac{\delta G_1}{\delta \bar{u}} + \Omega \frac{\delta G_2}{\delta \bar{u}} = \ddot{u} + \eta \dot{u} + -\frac{\partial^2 u}{\partial x^2} + 2\pi\gamma |u|^2 u - \mu u + i\Omega \frac{\partial u}{\partial x} = 0, \quad (35)$$

with the two Lagrange multiplicators from Eq. (B10)

$$\mu = \frac{b_1 E_{kin} - b_2 \ell}{N E_{kin} - \ell^2}, \quad \Omega = \frac{b_2 N - b_1 \ell}{N E_{kin} - \ell^2}. \quad (36)$$

In Eqs. (35) and (36) μ is the so called chemical potential, which is not equal to E for the NLSE, and Ω is the angular velocity for the rotation. The quantities N , E_{kin} , ℓ , b_1 , b_2 in Eq. (36), which depend on the fictitious time τ , are defined in Appendix B.

In Fig. 6 we have plotted the resulting so called Yrast curve (main figure) with the density and phase of the corresponding complex wave function u for the particularly interesting points $\ell_0 = 0, 0.5, 1$ (inset figures). At integer values of ℓ_0 (0, 1 in this example), u is a plane-wave $u = \exp(i\ell_0 x)/\sqrt{2\pi}$. At half-integer values (e.g. $\ell_0 = 0.5$), u corresponds to a dark solitary wave that circulates in the ring¹⁹, see the right-upper- and mid-lower-inset figures.

V. CONCLUSION

We have introduced the *dynamical functional particle method* (DFPM) with normalization and several orthogonalization constraints for the linear Schrödinger equation. Numerical results are presented for the wavefunctions and energies of the radial part of the hydrogen atom, and for the 2D harmonic oscillator. Furthermore, DFPM was formulated with constraints for rotational states to the non-linear Schrödinger equation and then solved numerically.

We believe this presentation of DFPM may be helpful for students and researchers who want to solve globally constrained equations in general. More specifically, it can be used for numerically solving different kinds of Schrödinger equations attaining (degenerated) excited states and energies.

ACKNOWLEDGMENTS

We acknowledge valuable comments from Patrik Sandin. We also thank the three “French musketeers” Julien Régnier, Nico Gaudy, and Alexandre Clercq for valuable discussions about DFPM during their internships at Örebro University.

Appendix A: Normalization constraint and several orthogonalization constraints

In the numerical examples in Sections IV A and IV B both a normalization constraint and several orthogonalization constraints are treated simultaneously. We here sketch how an arbitrary number of orthogonalization constraints are treated.

We generalize Eqs. (14) and (19) to a vector containing w orthogonalization constraints and one normalization constraint

$$\vec{G} = \begin{bmatrix} \int \bar{u}u_0 d\mathbf{x} \\ \int \bar{u}u_1 d\mathbf{x} \\ \vdots \\ \int \bar{u}u_{w-1} d\mathbf{x} \\ 1 - \int \bar{u}u d\mathbf{x} \end{bmatrix} = \vec{0}. \quad (\text{A1})$$

Hence with

$$\dot{\vec{G}} = \begin{bmatrix} \int \dot{\bar{u}}u_0 d\mathbf{x} \\ \int \dot{\bar{u}}u_1 d\mathbf{x} \\ \vdots \\ \int \dot{\bar{u}}u_{w-1} d\mathbf{x} \\ -\int \dot{\bar{u}}u + \bar{u}\dot{u} d\mathbf{x} \end{bmatrix}, \quad \ddot{\vec{G}} = \begin{bmatrix} \int \ddot{\bar{u}}u_0 d\mathbf{x} \\ \int \ddot{\bar{u}}u_1 d\mathbf{x} \\ \vdots \\ \int \ddot{\bar{u}}u_{w-1} d\mathbf{x} \\ -\int \ddot{\bar{u}}u + \bar{u}\ddot{u} + 2\dot{\bar{u}}\dot{u} d\mathbf{x} \end{bmatrix}, \quad (\text{A2})$$

we have from Eq. (13)

$$\ddot{\vec{G}} + \eta \dot{\vec{G}} = \begin{bmatrix} \int (\ddot{\bar{u}} + \eta \dot{\bar{u}}) u_0 d\mathbf{x} \\ \int (\ddot{\bar{u}} + \eta \dot{\bar{u}}) u_1 d\mathbf{x} \\ \vdots \\ \int (\ddot{\bar{u}} + \eta \dot{\bar{u}}) u_{w-1} d\mathbf{x} \\ -\int \{\ddot{\bar{u}} + \eta \dot{\bar{u}}\} u + \{\ddot{\bar{u}} + \eta \dot{\bar{u}}\} \bar{u} + 2\dot{\bar{u}}\dot{u} d\mathbf{x} \end{bmatrix} = \begin{bmatrix} -k_0 G_0 \\ -k_1 G_1 \\ \vdots \\ -k_{w-1} G_{w-1} \\ -k_w G_w \end{bmatrix}. \quad (\text{A3})$$

From Eq. (12) we now have

$$\ddot{\bar{u}} + \eta \dot{\bar{u}} = -\hat{H}\bar{u} - \sum_{j=0}^{w-1} \mu_j \bar{u}_j + \mu_w \bar{u}, \quad (\text{A4})$$

such that the left hand side of Eq. (A3) is

$$\ddot{\vec{G}} + \eta \dot{\vec{G}} = \begin{bmatrix} - \int u_0 \hat{H} \bar{u} d\mathbf{x} + \mu_w \int \bar{u} u_0 d\mathbf{x} - \sum_{j=0}^{w-1} \mu_j \int \bar{u}_j u_0 d\mathbf{x} \\ - \int u_1 \hat{H} \bar{u} d\mathbf{x} + \mu_w \int \bar{u} u_1 d\mathbf{x} - \sum_{j=0}^{w-1} \mu_j \int \bar{u}_j u_1 d\mathbf{x} \\ \vdots \\ - \int u_{w-1} \hat{H} \bar{u} d\mathbf{x} + \mu_w \int \bar{u} u_{w-1} d\mathbf{x} - \sum_{j=0}^{w-1} \mu_j \int \bar{u}_j u_{w-1} d\mathbf{x} \\ 2E + 2\mu_w (G_w - 1) + \sum_{j=0}^{w-1} \mu_j \int \bar{u}_j u d\mathbf{x} + \sum_{j=0}^{w-1} \mu_j \int \bar{u} u_j d\mathbf{x} - 2 \int \dot{u} \bar{u} d\mathbf{x} \end{bmatrix}. \quad (\text{A5})$$

Now since $\int \bar{u}_i u_j d\mathbf{x} = \delta_{ij}$ we can write Eq. (A3) on matrix form with the Lagrange multipliers as the unknowns

$$\begin{bmatrix} 1 & 0 & \dots & 0 & -G_0 \\ 0 & 1 & \dots & 0 & -G_1 \\ \vdots & \vdots & & \vdots & \vdots \\ 0 & 0 & \dots & 1 & -G_{w-1} \\ -\text{Re}(G_0) & -\text{Re}(G_1) & \dots & -\text{Re}(G_{w-1}) & 1 - G_w \end{bmatrix} \begin{bmatrix} \mu_0 \\ \mu_1 \\ \vdots \\ \mu_{w-1} \\ \mu_w \end{bmatrix} = \begin{bmatrix} k_0 G_0 - \int u_0 \hat{H} \bar{u} d\mathbf{x} \\ k_1 G_1 - \int u_1 \hat{H} \bar{u} d\mathbf{x} \\ \vdots \\ k_{w-1} G_{w-1} - \int u_{w-1} \hat{H} \bar{u} d\mathbf{x} \\ k_w G_w / 2 + E - \int |\dot{u}|^2 d\mathbf{x} \end{bmatrix}, \quad (\text{A6})$$

where $\text{Re}(G_j) = \int (\bar{u}_j u + \bar{u} u_j) d\mathbf{x} / 2$ and $E = \int \bar{u} \hat{H} u d\mathbf{x}$.

For example with only one ($w = 1$) orthogonality constraint, Eq. (A6) is the system in Eq. (23).

We note that the system (A6) can be solved very efficiently by sparse block Gaussian elimination with a computational cost proportional to w .

Appendix B: Normalization and angular momentum constraints

The two constraints we used for the NLSE are defined in Eq. (34). Taking the first and second order derivatives of G_1 and G_2 with respect to τ gives

$$\dot{G}_1 = - \int_{-\pi}^{\pi} (\dot{u} u + \bar{u} \dot{u}) dx, \quad \ddot{G}_1 = - \int_{-\pi}^{\pi} (\ddot{u} u + 2\dot{u} \dot{u} + \bar{u} \ddot{u}) dx, \quad (\text{B1})$$

respectively

$$\dot{G}_2 = i \int_{-\pi}^{\pi} \left(\dot{\bar{u}} \frac{\partial u}{\partial x} + \bar{u} \frac{\partial \dot{u}}{\partial x} \right) dx, \quad \ddot{G}_2 = i \int_{-\pi}^{\pi} \left(\ddot{\bar{u}} \frac{\partial u}{\partial x} + 2\dot{\bar{u}} \frac{\partial \dot{u}}{\partial x} + \bar{u} \frac{\partial \ddot{u}}{\partial x} \right) dx. \quad (\text{B2})$$

Inserting the expressions from Eqs. (B1) and (B2) into the left hand side of the general differential equation for constraints (13), then gives after simplifications

$$\ddot{G}_1 + \eta \dot{G}_1 = - \int_{-\pi}^{\pi} \left(\{ \ddot{u} + \eta \dot{u} \} u + \bar{u} \{ \ddot{u} + \eta \dot{u} \} + 2|\dot{u}|^2 \right) dx, \quad (B3)$$

and

$$\ddot{G}_2 + \eta \dot{G}_2 = i \int_{-\pi}^{\pi} \left(\{ \ddot{u} + \eta \dot{u} \} \frac{\partial u}{\partial x} + \bar{u} \left\{ \frac{\partial \ddot{u}}{\partial x} + \eta \frac{\partial \dot{u}}{\partial x} \right\} + 2\dot{u} \frac{\partial \dot{u}}{\partial x} \right) dx. \quad (B4)$$

The use of Eq. (35) for the curly brackets above gives (with η, γ, μ and Ω real, and by using integration by parts to some terms)

$$\ddot{G}_1 + \eta \dot{G}_1 = \int_{-\pi}^{\pi} \left(-2\bar{u} \frac{\partial^2 u}{\partial x^2} + 4\pi\gamma|u|^4 + 2i\Omega\bar{u} \frac{\partial u}{\partial x} - 2\mu|u|^2 - 2|\dot{u}|^2 \right) dx, \quad (B5)$$

and

$$\ddot{G}_2 + \eta \dot{G}_2 = \int_{-\pi}^{\pi} \left(2i \frac{\partial u}{\partial x} \frac{\partial^2 \bar{u}}{\partial x^2} - 2i\pi\gamma|u|^2 \bar{u} \frac{\partial u}{\partial x} - 2i\pi\gamma\bar{u} \frac{\partial (|u|^2 u)}{\partial x} + 2\Omega\bar{u} \frac{\partial^2 u}{\partial x^2} + 2i\mu\bar{u} \frac{\partial u}{\partial x} + 2i\dot{u} \frac{\partial \dot{u}}{\partial x} \right) dx. \quad (B6)$$

Comparing the above equations with Eq. (13) and inserting the constraints (34)

$$G_1 = 1 - \int_{-\pi}^{\pi} |u|^2 dx \equiv 1 - N = 0, \quad G_2 = \ell_0 + i \int_{-\pi}^{\pi} \bar{u} \frac{\partial u}{\partial x} dx \equiv \ell_0 - \ell = 0, \quad (B7)$$

with the three real functions $N(\tau)$, $\ell(\tau)$ and $E_{kin}(\tau) = - \int_{-\pi}^{\pi} \bar{u} \frac{\partial^2 u}{\partial x^2} dx$, being the norm, angular momentum, and kinetic energy, respectively, we have from Eq. (B5)

$$-2N\mu - 2\ell\Omega + \int_{-\pi}^{\pi} \left(-2\bar{u} \frac{\partial^2 u}{\partial x^2} + 4\pi\gamma|u|^4 - 2|\dot{u}|^2 \right) dx = -k_1 G_1, \quad (B8)$$

and from Eq. (B6)

$$-2\ell\mu - 2E_{kin}\Omega + \int_{-\pi}^{\pi} \left(2i \frac{\partial u}{\partial x} \frac{\partial^2 \bar{u}}{\partial x^2} - 4i\pi\gamma \frac{\partial u}{\partial x} |u|^2 \bar{u} - 2i\pi\gamma \frac{\partial (\bar{u}u)}{\partial x} \bar{u}u + 2i\dot{u} \frac{\partial \dot{u}}{\partial x} \right) dx = -k_2 G_2. \quad (B9)$$

The second to last term in the left hand side above disappears, since $\int \frac{\partial(\bar{u}u)}{\partial x} \bar{u}u dx = \int \frac{\partial}{\partial x} (\bar{u}u)^2 dx/2 = (|u(\pi)|^4 - |u(-\pi)|^4)/2 = 0$ due to the periodic boundary conditions.

Hence, Eqs. (B8) and (B9) leads us to the following linear system for the Lagrange multipliers

$$\begin{bmatrix} N & \ell \\ \ell & E_{kin} \end{bmatrix} \begin{bmatrix} \mu \\ \Omega \end{bmatrix} = \begin{bmatrix} k_1 G_1/2 + \int_{-\pi}^{\pi} \bar{u} \hat{H} u \, dx - \int_{-\pi}^{\pi} |\dot{u}|^2 \, dx \\ k_2 G_2/2 - i \int_{-\pi}^{\pi} \frac{\partial u}{\partial x} \hat{H} \bar{u} \, dx + i \int_{-\pi}^{\pi} \bar{u} \frac{\partial \dot{u}}{\partial x} \, dx \end{bmatrix} \equiv \begin{bmatrix} b_1 \\ b_2 \end{bmatrix}, \quad (\text{B10})$$

where $\hat{H}u = \delta E / \delta \bar{u}$ with E from Eq. (33). Using Cramer's rule on the above linear system gives the explicit expressions used in Eq. (36).

* magnus.ogren@oru.se

† marten.gulliksson@oru.se

¹ As a starting point for own coding, see supplemental material at <http://dx.doi.org/XX.XXXX/XX.XXXXXXXX> [URL will be inserted by AIP], **TEMPORARY supplemental material for the reviewers can be found as ancillary files in the Arxiv, i.e. search for this article at <https://arxiv.org/>.**, including: a simplified MATLAB program *DFPM_1D_HO.m* that can calculate excited states of a particle in a 1D harmonic oscillator potential; and an XML input file *DFPM_1D_HO_1st_excited_state.xmds* for the free software www.xmds.org that can be used to solve the same problem for the first excited state; and a simplified MATLAB program *DFPM_1D_NLSE.m* that solves the NLSE as described in this article.

² M. Gulliksson, M. Ögren, A. Oleynik, Y. Zhang (2018), “Damped Dynamical Systems for Solving Equations and Optimization Problems”. In: Sriraman B. (eds) Handbook of the Mathematics of the Arts and Sciences. Springer, Cham.

³ I. M. Gelfand, S. V. Fomin, “Calculus of Variations”, Dover, New York (2000), ISBN 0-486-41448-5.

⁴ P. Begout, J. Bolte, M. Jendoubi, “On damped second-order gradient systems”, Journal of Differential Equations **259**, 3115 (2015).

⁵ E. Hairer, C. Lubich, and G. Wanner. “Geometric Numerical Integration”, 2nd ed. Springer (2006), ISBN 978-3-540-30666-5.

⁶ M. Gulliksson, “The Discrete Dynamical Functional Particle Method for Solving Constrained Optimization Problems”, Dolomites Research Notes on Approximation **10**, 6 (2017).

⁷ M. Gulliksson, S. Edvardsson, A. Lind, “The Dynamical Functional Particle Method”, arXiv:1303.5317.

⁸ B. T. Poljak, “Some methods of speeding up the convergence of iterative methods”, Akademija Nauk SSSR. Zurnal Vycislitel nli Matematiki i Matematicoskoi Fiziki **4**, 791 (1964).

⁹ I. Sandro, P. Valerio, Z. Francesco, “A New Method for Solving Nonlinear Simultaneous Equations”, SIAM Journal on Numerical Analysis **16**, 779 (1979).

¹⁰ G. Smyrlis, V. Zisis, “Local convergence of the steepest descent method in Hilbert spaces”, Journal of Mathematical Analysis and Applications **300**, 436 (2004).

¹¹ D. V. Schroeder, “The variational-relaxation algorithm for finding quantum bound states”, Am. J. Phys. **85**, 698 (2017).

¹² P. Sandin, M. Ögren, M. Gulliksson, “Numerical solution of the stationary multicomponent nonlinear Schrödinger equation with a constraint on the angular momentum”, Phys. Rev. E **93**, 033301 (2016).

¹³ P. C. Chow, “Computer Solutions to the Schrödinger Equation”, Am. J. Phys. **40**, 730 (1972); *ibid*, J. S. Bolemon, “Computer Solutions to a Realistic “One-Dimensional” Schrödinger Equation”, 1511.

¹⁴ P. J. Cooney, E. P. Kanter, Z. Vager, “Convenient numerical technique for solving the onedimensional Schrödinger equation for bound states”, Am. J. Phys. **49**, 76 (1981); K. Randles, D. V. Schroeder, B. R. Thomas, “Quantum matrix diagonalization visualized”, Am. J. Phys. **87**, 857 (2019).

¹⁵ R. McLachlan, K. Modin, O. Verdier, M. Wilkins, “Geometric generalisations of SHAKE and RATTLE”, Foundations of Computational Mathematics **14**, 339 (2014).

¹⁶ L. I. Schiff, “quantum mechanics”, 3.rd ed., Mc Graw-Hill, ISBN 0-07-Y85643-5.

¹⁷ M. Abramowitz, I. A. Stegun (eds.), “Handbook of Mathematical Functions”, National Bureau of Standards Publication, 1964.

¹⁸ C. J. Pethick, H. Smith, “Bose-Einstein Condensation in Dilute Gases”, second edition, Cambridge 2008.

¹⁹ A. D. Jackson, J. Smyrnakis, M. Magiopoulos, G. M. Kavoulakis, “Solitary waves and yrast states in Bose-Einstein condensed gases of atoms”, Europh. Lett., **95**, (2011) 30002.